BES-MEMO
Haiwen Zhao
Jun.1,1997

Measurement of D-meson Production Cross Section in e^+e^- Annihilation at Ec.m.=4.03 GeV

BES Collaboration
Institute of High Energy Physics, Beijing

Abstract

The data collected with the BES detector at BEPC at a center-of-mass energy 4.03 GeV, which correspond to an integrated luminosity of 22.3 pb^{-1}, were analyzed. D^0, $\bar{D}^0$ and $D^{\pm}$ were reconstructed from $K^{\mp}\pi^{\pm}$ and $K^{\mp}\pi^{\pm}\pi^{\pm}$ decay modes. The inclusive production cross sections of D^0 and $\bar{D}^0$, $D^{\pm}$, and the exclusive production cross section of $e^+e^- \rightarrow D\bar{D}$, $\bar{D}D^*$ or $D\bar{D}^*$, and $D^*\bar{D}^*$ pairs have been measured. A comparison of the measurement results with the coupled-chennel model are also presented.

Typeset using REVTEX

I. INTRODUCTION

One of the most noticable phenomena in e^+e^- annihilation is that the value of R (ratio of the hadronic to muon-pair cross sections) exhibits a complex energy dependance associated with the production of charmed particles at energies above the prominent ψ and ψ' peaks. The production of charmed mesons has been studied in many experiments at the ψ'' and higher energies and many properties of D and D^* were determined [1 - 5]. The production of charmed mesons was also predicted theoretically by coupled-chennel model [6,7]. More measurements with large data set are still nessesary and tests for this model are still required.

In this paper, we report a measurement of D and D^* production cross section at 4.03 GeV. The analysis is based on $22.3pb^{-1}$ of data from e^+e^- collisions at a centr-of-mass energy 4.03 GeV, taken with the BES detector during the 1992-1994 BEPC run.

The BES is a conventional cylindrical detector, which is described in detail in Ref.[8]. A four-layer central drift chamber (CDC) surrounding the beampipe provides trigger information. Outside the CDC, a ten-layer main drift chamber (MDC) provides tracking and energy loss(dE/dx) information on charged tracks over $\sim 85\%$ of the total solid angle. The momentum resolution is $\sigma_p/p = 0.017\sqrt{1+p^2}$ (p in GeV/c), and the energy loss (dE/dx) resolution is $\sim 11\%$ for hadron tracks and $\sim 8.5\%$ for Bhabha electrons. Scintillation counters which surround the MDC provide time-of-flight (TOF) measurements, with resolutions of $\sim$ 450 ps for hadrons and $\sim$ 330 ps for Bhabha events. Outside the TOF system a 12-radiation-length, lead-gas barrel shower counter (BSC), operating in limited streamer mode, measures the energies of electrons and photons over $\sim 80\%$ of the total solid angle,and achieves energy resolution $\sigma_E/E = 0.22/\sqrt{E}$ (E in GeV) for electrons, and spatial resolutions σ_ϕ=4.5 mrad and σ_z=2 cm. A solenoidal magnet provides a 0.4 T magnetic field in the central tracking region of the detector. Three double-layer muon counters (MUC) instrument the magnet flux return, and serve to identify muons of momentum greater than 0.5 GeV/c. They cover $\sim 68\%$ of the total solid angle with longitudinal (transverse) spatial resolution of 5 cm (3 cm).

We describe the measurement of D-meson production in Section II. And, in Section III, the rates of the exclusive cross sections are compared with that of predicted theoretically by model of Eichten *et al.*

II. PRODUCTION CROSS SECTION OF D AND D^*

At $\sqrt{E} = 4.03$ GeV, the charmed mesons $D^\pm$, D^0, $\bar{D}^0$, and $Ds^\pm$ are produced. Comparing with D, the cross section of Ds is small. The D production proceeds by the following reactions

(a) $e^+e^- \to D\bar{D}$

(b) $e^+e^- \to D^*\bar{D}$ or $\bar{D}^*D$

(c) $e^+e^- \to D^*\bar{D}^*$

Besides these, nonresonant production $D\bar{D}\pi$, $D\bar{D}\pi\pi$, and initial state radiation $e^+e^- \to \gamma\psi(3s)$, followed by $\psi(3s) \to D\bar{D}$ are allowed kinematically and are in principle possible. Since the threshold of D^* production is very close to $\sqrt{E} = 4.03$ GeV, the nonresonant production is expected to be negligible if not zero. In the rest of this paper, nonresonant cross section will be assumed to be zero. The only contributions of $D^{\pm}$ and $D^0\ \bar{D}^0$ are from reaction (a), (b), (c).

Reaction (a) includes $e^+e^- \to D^0\bar{D}^0$ and $e^+e^- \to D^+D^+$; (b) includes $e^+e^- \to D^{\pm}D^{*\mp}$, $e^+e^- \to D^0\bar{D}^{*0}$ or $\bar{D}^0D^{*0}$; Reaction (c) performs $e^+e^- \to D^{*\pm}D^{*\mp}$, $e^+e^- \to D^{*0}\bar{D}^{*0}$. Vector meson D^{*+} subsequently decays to $D^+\gamma$, $D^+\pi^0$ or $D^0\pi^+$; and,D^{*0} decays to $D^0\gamma$ or $D^0\pi^0$.

D-mesons used in this analysis were reconstructed from the decay modes $D^0 \to K^-\pi^+$, $\bar{D}^0 \to K^+\pi^-$ and $D^{\pm} \to K^{\mp}\pi^{\pm}\pi^{\pm}$. These modes have a better ratio of signal to background in the invariant-mass distributions than other decay chennels. Well-reconstructed charged tracks (MFIT=2,-9,-19) were used to combine in reconstruction. Tracks are required to come within 1 cm radialy and within ± 15 cm longitudinally of the measured beam crossing point. The polar angle of charged track θ is required to satisfy $|cos\theta| \leq 0.80$ to provide reliable tracking and barrel TOF information. The dE/dx and TOF information of a charged track are used to identify a charged particle. They are required to be consistent with the mass hypothesis assigned to the track. The confidence level of a track for each particle hypothesis e, μ, π, K and proton P are defined as $CL_i = 1 - Prob(\chi_i^2)$, where $Prob(\chi_i^2)$ is the probability of the χ^2 distribution for each partical hypothesis and i denotes e, μ, π, K or P. χ_i^2 is the joint chi-square of the available dE/dx and TOF information for the track, defined as $\chi_i^2 = \chi_i^2(TOF) + \chi_i^2(dE/dx)$, where $\chi_i^2(TOF) = (t - t_i)^2/\sigma_{TOF}^2$, t is the measured time of flight and t_i is expected time of flight for i particle hypothsis. σ_{TOF}^2 is the resolution of TOF. In the same sense, we have $\chi_i^2(dE/dx) = (dE/dx - dE/dx_i)^2/\sigma_{dE/dx}^2$. In particle identification, $CL_K > 0.01$ and $W_K/(W_K + W_\pi) > 0.5$ are required for K candidate; $CL_\pi > 0.01$ and $W_K/(W_K + W_\pi) \leq 0.5$ for π candidate, where $W_K = exp(-\chi_K^2(TOF)/2) \cdot exp(-\chi_K^2(dE/dx)/2)$ and $W_\pi = exp(-\chi_\pi^2(TOF)/2) \cdot exp(-\chi_\pi^2(dE/dx)/2)$. Besides these, the measured momentum of each track is corrected for dE/dx losses in material traversed, according to what particle it is, and for a shift of BES magnetic field.

Signals of $D^{\pm}$, D^0 and $\bar{D}^0$ are observed as peaks in the invariant-mass spectra of $K^{\mp}\pi^{\pm}$ and $K^{\mp}\pi^{\pm}\pi^{\pm}$ as shown in Fig.1. The mass means and widths obtained from the fits to a Gaussian plus a polynominal background are 1866.5 $\pm$ 0.8 MeV and 26.5 $\pm$ 0.9 MeV for $K^{\mp}\pi^{\pm}$ mode; 1868.9 $\pm$ 0.9 MeV and 20.9 $\pm$ 1.1 MeV for $K^{\mp}\pi^{\pm}\pi^{\pm}$ mode. Monte Carlo study and data both indicate that the momentum of D^+ or D^0 which come from reactions (a), (b) and (c) are quite different and they seperate well (see Table I). Fig.2 shows the momentum distributions of $K^{\mp}\pi^{\pm}$ and $K^{\mp}\pi^{\pm}\pi^{\pm}$ under a cut of $|M_{K\pi} - 1866.6| \leq 79.5$ MeV (2σ) and $|M_{K\pi\pi} - 1868.7| \leq 62.7$ MeV (3σ) respectively. According to its momentum one can determine from which reacation a reconstructed D comes.

The amounts of $D^{\pm}$, D^0 and $\bar{D}^0$ were determined by fitting the invariant-mass distributions to a Gaussian function plus a polynomal background. Numbers of tagged $D^{\pm}$, $D^0(\bar{D}^0)$ produced from reactions (a), (b), (c) were determined by fitting the inariant-mass distribution under the approprate cuts on momenta (see Table II and Fig.3).

In the calculation of the production cross sections, efficences of reconstruction are needed. There are totally eight event types for D^0 and six types for D^+ in the D production at Ec.m.=4.03 GeV. The reconstruction efficences via $K^-\pi^+\pi^+$ and $K^-\pi^+$ for each event type, as listed in Table III, are determined by Monte Carlo study. Simulation events are generated in the way that one meson of the pairs decays to specific chennal, whereas the other one decays to cocktail.

For convenience we denote $br^+ = BR(D^+ \to K^-\pi^+\pi^+)$, $br^0 = BR(D^0 \to K^-\pi^+)$,

$b_1 = BR(D^{*+} \to D^+\gamma)$, $b_2 = BR(D^{*+} \to D^+\pi^0)$, $b_3 = BR(D^{*+} \to D^0\pi^+)$, $b_1^0 = BR(D^{*0} \to D^0\gamma)$ and $b_2^0 = BR(D^{*0} \to D^0\pi^0)$. In the following calculations, from Ref.[9], we have $br^+ = 9.1 \pm 0.6\%$, $br^0 = 3.83 \pm 0.12\%$, $b_1 = 1.1^{+2.1}_{-0.7}\%$, $b_2 = 30.6 \pm 2.5\%$, $b_3 = 68.3 \pm 1.4\%$, $b_1^0 = 38.1 \pm 2.9\%$ and $b_1^0 = 61.9 \pm 2.9\%$.

In the determining of cross sections, contributions of revalent event types to each production process are considered. In the reaction of $e^+e^- \to D\bar{D}$, the numbers of tagged D^+ and D^0 can be written as follows:

$$N_{D^0} = L \cdot \sigma(D^0\bar{D}^0) \cdot \varepsilon_1^0 \cdot br^0 \tag{1}$$

$$N_{D^+} = L \cdot \sigma(D^+D^-) \cdot \varepsilon_1 \cdot br^+ \tag{2}$$

where the integreted luminosity $L = 22.3\ pb^{-1}$ (obtained by BhaBha scattering events); $\sigma(D^+D^-)$ and $\sigma(D^0\bar{D}^0)$ are the exclusive production cross sections $e^+e^- \to D^+D^-$ and $e^+e^- \to D^0\bar{D}^0$ respectively; ε_1 and ε_1^0 are efficiencies of associated event type.

The inclusive production cross sections of D^+ and D^0 come from this mode can be calculated as

$$\sigma(D^0) = \sigma(D^0\bar{D}^0) \tag{3}$$

$$\sigma(D^+) = \sigma(D^+D^-). \tag{4}$$

In the reaction of $e^+e^- \to DD^*$ or $\bar{D}D^*$, we have

$$N_{D^+} = L \cdot \sigma(D^+D^{*-}) \cdot (\varepsilon_2 + \varepsilon_3 \cdot b_1 + \varepsilon_4 \cdot b_2) \cdot br^+ \tag{5}$$

$$N_{D^0} = L \cdot \sigma(D^0\bar{D}^{*0}) \cdot (\varepsilon_2^0 + \varepsilon_3^0 \cdot b_1^0 + \varepsilon_4^0 \cdot b_2^0) \cdot br^0 + L \cdot \sigma(D^+D^{*-}) \cdot \varepsilon_5^0 \cdot b_3 \cdot br^0 \tag{6}$$

and then there are

$$\sigma(D^+) = (1 + b_1 + b_2) \cdot \sigma(D^+D^{*-}) \tag{7}$$

$$\sigma(D^0) = b_3 \cdot \sigma(D^+D^{*-}) + 2 \cdot \sigma(D^0\bar{D}^{*0}) \tag{8}$$

In the reaction of $e^+e^- \to D^*\bar{D}^*$, we have

$$N_{D^+} = L \cdot \sigma(D^{*+}D^{*-}) \cdot (\varepsilon_5 \cdot b_1 + \varepsilon_6 \cdot b_2) \cdot br^+ \tag{9}$$

$$N_{D^0} = L \cdot \sigma(\bar{D}^{*0}D^{*0}) \cdot (\varepsilon_6^0 \cdot b_1^0 + \varepsilon_7^0 \cdot b_2^0) \cdot br^0 + L \cdot \sigma(D^{*+}D^{*-}) \cdot \varepsilon_8^0 \cdot b_3 \cdot br^0 \tag{10}$$

then we get

$$\sigma(D^+) = (b_1 + b_2) \cdot \sigma(D^{*+}D^{*-}) \tag{11}$$

$$\sigma(D^0) = \sigma(D^{*0}\bar{D}^{*0}) + b_3 \cdot \sigma(D^{*+}D^{*-}) \tag{12}$$

By Substituting the values of numbers of single tagged D^+ and D^0 (See Table II, becaues of charge conjugation, we have $N_{D^+} = N_{D^\pm}/2$, and $N_{D^0} = (N_{D^0} + N_{\bar{D}^0})/2$) for each production mode, branching fraction values and efficiencies for each event type (See Table III, For the $D\bar{D}$ case, we used $\varepsilon_1^0 = 0.232$ and $\varepsilon_1 = 0.211$, which are the efficiencies under momenta cuts), cross sections can be obtained from the equations (1)-(12). The results are listed as in Table IV and Table V. The first item of error is the statistic error caused by statistic uncertainty of ΔN_D. The second item of error is systematic error due to the uncertainty of branching fractions, a variation of luminosity L by 2.5% and the uncertainty of N_D via varying the background function and fit range in the invariant-mass fitting. The systematic error caused by the uncertainty of efficiences are not included. A variation of average efficiences by 10% will cause a change of inclusive D cross section by 10%.

III. CONCLUSION

It is a good test on Coupled-channel model in the 3.9 - 4.1 GeV region to measure the ratios of $D\bar{D}$ to DD^* exclusively.

In this analysis, raditive process may have contribution to lower side of the momentum distribution of $D^\pm$ between 0.334 GeV to 0.668 GeV. Monte carlo study indicate that the energy of most of initial state radiative photons is less than 80 MeV. That means at $\sqrt{E} =$ 4.03 GeV, even though the initial state radiation exists, the rest energy is still over the threshold of $D^\pm D^{*\mp}$, $D^\pm D^{*\mp}$ pairs may be produced and $\sigma(D^\pm D^{*\mp})$ is valid.

Coupled-channel model predicts the rate of charm production cross sections[6] at $\psi(4028)$ to be:
$R_{(D^{*0}\bar{D}^{*0})} : R_{(D^0\bar{D}^{*0}+\bar{D}^0 D^{*0})} : R_{(D^0\bar{D}^0)} = 1.0 : 1.35 : 0.005$
$R_{(D^{*+}D^{*-})} : R_{(D^+D^{*-}+D^-D^{*+})} : R_{(D^+D^-)} = 1.0 : 2.69 : 0.004$

SLAC-LBL gave a measurement[4] at $\psi(4028)$ that:
$R_{(D^{*0}\bar{D}^{*0})} : R_{(D^0\bar{D}^{*0}+\bar{D}^0 D^{*0})} : R_{(D^0\bar{D}^0)} = (1.0 \pm 0.10) : (0.85 \pm 0.09) : (0.10 \pm 0.06)$
The rates of charged D cross sections were not given.

In this experiment, we can give the rates as follows:
$R_{(D^{*0}\bar{D}^{*0})} : R_{(D^0\bar{D}^{*0}+\bar{D}^0 D^{*0})} : R_{(D^0\bar{D}^0)} = (1.00 \pm 0.15) : (1.41 \pm 0.23) : (0.11 \pm 0.04)$
$R_{(D^{*+}D^{*-})} : R_{(D^+D^{*-}+D^-D^{*+})} : R_{(D^+D^-)} = (1.00 \pm 0.19) : (1.98 \pm 0.19) : (0.16 \pm 0.04)$

We found the rate of neutral D are in good agreement with coupled-channel model whereas, the rate of charged D has some difference.

We would like to thank the staffs of the BEPC accelerator and the Computing Center at the Institute of High Energy Physics (Beijing).

REFERENCES

[1] R.H.Schindler *et.al.*, Phys. Rev. D **24**, 78 (1981).
[2] A.Rapidis *et.al.*, Phys. Rev. Lett. **24**, 526 (1977).
[3] M.Piccolo *et.al.*, Phys. Lett. **86B**, 220 (1979).
[4] G.Goldhaber *et. al.*, Phys. Lett. **69B**, 503 (1977).
[5] MarK II Collaboration, M. W. Coles *et. al.*, Phys. Rev. D **26**, 2190 (1982).
[6] E. Eichten *et.al.*, Phys. Rev. D **21**, 227 (1980).
[7] E. Eichten *et.al.*, Phys. Rev. D **17**, 3090 (1978).
[8] J. Z. Bai *et. al.*, Nucl. Instr. and Methods **A344**, 319 (1994); J. Z. Bai *et. al.*, Phys. Rev. Lett. **69**, 3021 (1992);
[9] Particle Dara Group, Phys. Rev. D **54**, 1 (1996).

TABLES

TABLE I. Momenta range for production modes

production mode	theoreticl momenta	experimental momenta
$e^+e^- \to D^*\bar{D}^*$	0.004-0.308 GeV	0.0-0.34 GeV
$e^+e^- \to D^*\bar{D}$ or $\bar{D}^*D$	0.368-0.664 GeV	0.34-0.70 GeV
$e^+e^- \to D\bar{D}$	P_{D^+}:0.752, P_{D^0}:0.764 GeV	0.70-0.80 GeV

TABLE II. Events number for each production mode ($P_D : GeV$)

		Event number $N_D + N_{\bar{D}}$		
channel	$e^+e^- \to D^*\bar{D}^*$	$e^+e^- \to D^*\bar{D}(\bar{D}^*D)$	$e^+e^- \to D\bar{D}$	total
cut	$p_D < 0.34$	$0.34 < P_D < 0.70$	$0.725 < P_{D^+} < 0.775$	
			$0.742 < P_{D^0} < 0.788$	
$D^0 \to K^-\pi^+$	$1648 \pm 78 \pm 31$	$2022 \pm 110 \pm 198$	$82 \pm 26 \pm 8$	$3752 \pm 137 \pm 200$
$D^+ \to K^-\pi^+\pi^+$	$456 \pm 64 \pm 6$	$1774 \pm 118 \pm 11$	$168 \pm 38 \pm 2$	$2398 \pm 139 \pm 12$

TABLE III. Efficence for each event type

event type	efficiency (%)
$e^+e^- \to D^+D^-$, direct D	$\varepsilon_1 = 0.281$
$e^+e^- \to D^+D^{*-}$, direct D	$\varepsilon_2 = 0.273$
$e^+e^- \to D^-D^{*+}$, $D^{*+} \to D^+\gamma$	$\varepsilon_3 = 0.265$
$e^+e^- \to D^-D^{*+}$, $D^{*+} \to D^+\pi^0$	$\varepsilon_4 = 0.272$
$e^+e^- \to D^{*-}D^{*+}$, $D^{*+} \to D^+\gamma$	$\varepsilon_5 = 0.293$
$e^+e^- \to D^{*-}D^{*+}$, $D^{*+} \to D^+\pi^0$	$\varepsilon_6 = 0.288$
$e^+e^- \to D^0\bar{D}^0$, direct D^0	$\varepsilon_1^0 = 0.359$
$e^+e^- \to D^0\bar{D}^{*0}$, direct D^0	$\varepsilon_2^0 = 0.359$
$e^+e^- \to \bar{D}^0D^{*0}$, $D^{*0} \to D^0\gamma$	$\varepsilon_3^0 = 0.356$
$e^+e^- \to \bar{D}^0D^{*0}$, $D^{*0} \to D^0\pi^0$	$\varepsilon_4^0 = 0.349$
$e^+e^- \to D^-D^{*+}$, $D^{*+} \to D^0\pi^+$	$\varepsilon_5^0 = 0.322$
$e^+e^- \to \bar{D}^{*0}D^{*0}$, $D^{*0} \to D^0\gamma$	$\varepsilon_6^0 = 0.381$
$e^+e^- \to \bar{D}^{*0}D^{*0}$, $D^{*0} \to D^0\pi^0$	$\varepsilon_7^0 = 0.318$
$e^+e^- \to D^{*-}D^{*+}$, $D^{*+} \to D^0\pi^+$	$\varepsilon_8^0 = 0.402$

TABLE IV. Inclusive production cross sections of D^+ and D^0 (charge conjugation included)

production mode	$\sigma(D^0)$	$\sigma(D^+)$
$e^+e^- \to D^*\bar{D}^*$	$5.35 \pm 0.45 \pm 0.44$ nb	$0.78 \pm 0.11 \pm 0.13$ nb
$e^+e^- \to D\bar{D}^*$	$6.82 \pm 0.39 \pm 0.77$ nb	$3.21 \pm 0.21 \pm 0.24$ nb
$e^+e^- \to D\bar{D}$	$0.41 \pm 0.13 \pm 0.04$ nb	$0.39 \pm 0.09 \pm 0.03$ nb
Total	$12.58 \pm 0.61 \pm 0.89$ nb	$4.38 \pm 0.26 \pm 0.27$ nb

TABLE V. Exclusive production cross section for each mode

production mode	cross section
$e^+e^- \to D^{*+}D^{*-}$	$\sigma(D^{*+}D^{*-}) = 1.23 \pm 0.17 \pm 0.16$ nb
$e^+e^- \to D^{*0}\bar{D}^{*0}$	$\sigma(D^{*0}\bar{D}^{*0}) = 1.83 \pm 0.19 \pm 0.19$ nb
$e^+e^- \to D^{\pm}D^{*\mp}$	$\sigma(D^{\pm}D^{*\mp}) = 2.44 \pm 0.16 \pm 0.17$ nb
$e^+e^- \to \bar{D}^0D^{*0}$ or $D^0\bar{D}^{*0}$	$\sigma(\bar{D}^0D^{*0}$ & $D^0\bar{D}^{*0}) = 2.58 \pm 0.19 \pm 0.38$ nb
$e^+e^- \to D^+D^-$	$\sigma(D^+D^-) = 0.20 \pm 0.04 \pm 0.01$ nb
$e^+e^- \to D^0\bar{D}^0$	$\sigma(D^0\bar{D}^0) = 0.21 \pm 0.07 \pm 0.02$ nb

FIGURES

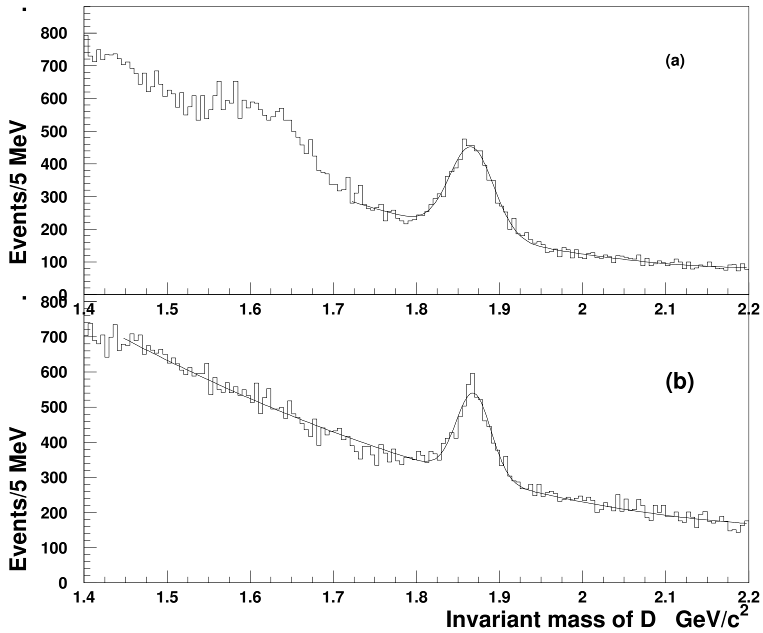

FIG. 1. Invariarant mass distribution for (a). $D^0 \to K^-\pi^+$, (b). $D^+ \to K^-\pi^+\pi^+$

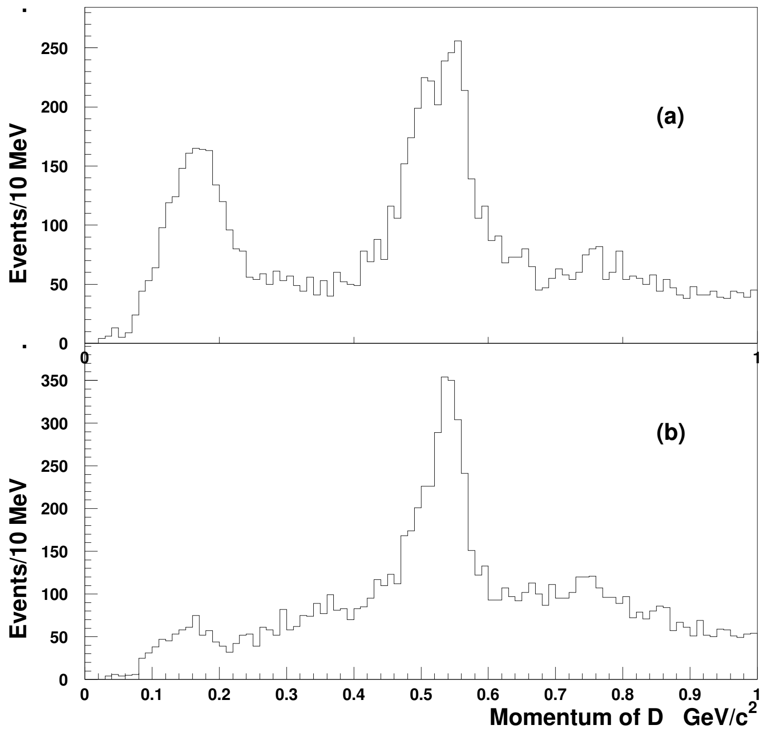

FIG. 2. Momenta distribution for (a). $D^0 \to K^-\pi^+$ and (b). $D^+ \to K^-\pi^+\pi^+$

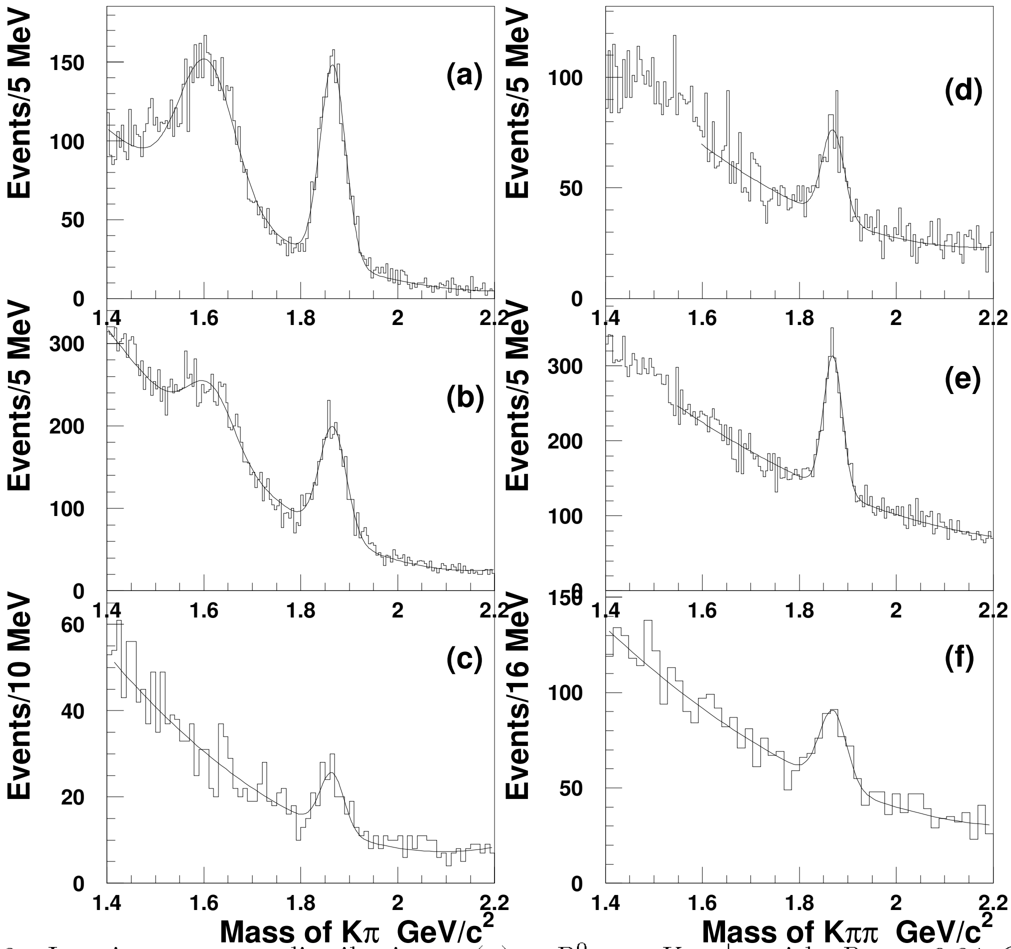

FIG. 3. Invariarant mass distribution. (a). $D^0 \to K^-\pi^+$, with $P_D < 0.34$ GeV. (b). $D^0 \to K^-\pi^+$, with 0.34 GeV $\leq P_D <$ 0.70 GeV. (c). $D^0 \to K^-\pi^+$, with 0.742 GeV $\leq P_D <$ 0.788 GeV ($\pm 1\sigma$). (d). $D^+ \to K^-\pi^+\pi^+$, with $P_D < 0.34$ GeV. (e). $D^+ \to K^-\pi^+\pi^+$, with 0.34 GeV $\leq P_D <$ 0.70 GeV. (f). $D^+ \to K^-\pi^+\pi^+$, with 0.725 GeV $\leq P_D <$ 0.775 GeV.